# Robust PET Motion Correction Using Non-local Spatio-temporal Priors

S. Thiruvenkadam[1], K.S. Shriram[1], R. Manjeshwar[2], and S.D. Wollenweber[3]

[1] GE Global Research, Bangalore, India
[2] GE Global Research, Niskayuna, USA
[3] GE Healthcare, Waukesha, USA

**Abstract.** Respiratory motion presents significant challenges for PET/CT acquisitions, potentially leading to inaccurate SUV quantitation. Non Rigid Registration [NRR] of gated PET images is quite challenging due to large motion, intrinsic noise, and the need to preserve definitive features like tumors. In this work, we use non-local spatio-temporal constraints within group-wise NRR to get a stable framework which can work with few number of PET gates, and handle the above challenges of PET data. Additionally, we propose metrics for measuring alignment and artifacts introduced by NRR which is rarely addressed. Our results are quantitatively compared to related works, on 20 clinical PET cases.

## 1 Introduction

Patient respiratory motion is a key challenge for PET/CT imaging, which could lead to blurring of clinically definitive features such as tumors. Such blurring in turn affects detectability of tumors, accuracy of SUV values, and could lead to sub-optimal radiation therapy planning. Motion compensation can be done by factoring in CT/MR derived motion fields within PET reconstruction [1] or using joint frameworks for motion/attenuation correction [2]. An alternative approach is to reconstruct, non-rigidly register and then average [RRA] to get a higher SNR PET image [3, 4]. Although the more sophisticated approaches where motion compensation is treated within reconstruction such as [1, 2] are theoretically preferable, the RRA method is simpler from a computational perspective. In this work, we address PET motion correction within the RRA framework.

Fundamentally, this is the problem of non-rigidly aligning multiple 3D images. The '*reference*' based approach as in [3, 4] would be to pick one of the images as reference and non-rigidly register the other images to it. Alternatively, one could use *groupwise* NRR. Unlike pairwise formulations, group wise motion correction is 'reference free' and is not biased by the choice of the reference image. In gated PET data, reconstruction artifacts e.g. due to PET-CT phase mismatch or incorrect gating may occur in some of the gates. Thus, pronounced differences in registration results occur with a different choice of the reference image.

Groupwise NRR [5–8] is used for aligning large populations of data without the problem of reference bias. Simply put, group-wise registration iteratively


N. Navab et al. (Eds.): MICCAI 2015, Part II, LNCS 9350, pp. 643–650, 2015.
DOI: 10.1007/978-3-319-24571-3_77

estimates the 'reference image' and the transforms to map the images to the reference domain. The issue however is, the bare groupwise NRR formulation is unstable and additional constraints are essential for stability especially for NRR of small populations. Current works have enhanced groupwise NRR using spatial constraints on the deformation [5,6], temporal constraints [9] and feature based metrics [8]. Additionally, NRR of gated PET images is quite challenging due to large motion, intrisic noise, and the need to preserve small features like tumors. Large motion impacts structures such as small tumors leading to collapse, splits etc. resulting in quantitation inaccuracies. Thus, group-wise NRR in addition to handling the stabilty issue, has to robustly handle above data challenges.

Many of the previous groupwise NRR efforts have been in Atlas building where these efforts typically work with large populations and there is no correlation of motion expected across the population. The main challenge these works have tried to address is multiple modes of variation in the population. However, the problem here is different, gated PET data has frequently as few as 4 to 6 gates. Thus, standard groupwise NRR formulations are unstable since, even locally, there might be multiple solution pairs for the jointly estimated reference image and transforms. Also, in 4D data having respiratory/cardiac motion, there is strong correlation of motion across frames and across faraway regions. For example, the effects of respiration can be seen as low as the pelvic region. The above motion correlation, if modeled, could be effective in tackling the instability issue of groupwise NRR, and the large motion/noise challenges of PET data. Although not completely representative, non-local penalties on the motion fields come close in modeling such correlations between faraway regions. Non-local regularization ( [10], [11]) of the motion fields is shown to give increased robustness to large motion, noise, and small structures compared to local approaches.

In this work, we propose non-local spatio-temporal constraints within groupwise NRR to get a stable 4D framework which can also handle above challenges of PET data. The non-local penalties differentiates our work from above prior groupwise NRR works, and is key in robust prediction of definitive PET features under large motion. The reasoning is that at a location where a small structure exhibits large motion, a non-local neighbour such as lung/cardiac interface where it is easier to capture the motion, can help in predicting the structure's motion. We also carefully address the important aspect of NRR validation using lesion profile based metrics. These metrics measure two aspects of NRR quality, namely, alignment and artifacts. Alignment is a common attribute that is measured in Registration works. Here, we additionally propose measures for artifacts introduced by NRR which is rarely addressed. We compare our results to level set NRR which is part of ITK (Vemuri et al. [12], used for PET motion correction [4]) and a Groupwise NRR algorithm similar to [6].

## 2 Methods

We assume a monomodal scenario since large intensity changes are not expected in gated PET data. Intensity/contrast changes that could occur e.g. due to gating

induced count variations, can be handled using preprocess normalization steps. Given $N$ PET gates $\{I_k\}_{k=1}^N$ defined on $\Omega$, we seek a reference image $\mu$ and deformation fields $\{u_k\}_{k=1}^N$, $\mathbf{u} = [u_1, u_2, ..., u_N]$, which minimizes:

$$E[\mu, \mathbf{u}] = \sum_{k=1}^{N} \int_{\Omega} |I_k(. + u_k) - \mu|^2 dx + \lambda \int_{\Omega} |\nabla u_k|^2 dx \tag{1}$$

The above objective function [**GW**] is the basic formulation of groupwise NRR, posed on smooth motion fields and measures pixel level variance of the PET images. [**GW**] can be minimized by iteratively updating $\mu = \frac{1}{N} \sum_{k=1}^{N} I_k(. + u_k)$ and motion fields $\mathbf{u}$. It is however seen that the above formulation is illposed since there might be, even locally, several solutions of $\mu, \mathbf{u}$ with the same energy $E$. One way to address this instability is to use a penalty that seeks, $\sum_{k=1}^{N} \int_{\Omega} u_k dx = 0$ as in [6], which is called the '*zero deformation*' penalty. We refer to the Groupwise NRR framework with the zero deformation penalty as [**GW-zD**].

As highlighted in the introduction, we augment Eq. 1 with non-local spatio-temporal penalties to give a stable framework, able to handle the data challenges of PET modality. Specifically, we look at proposed energy [**GW-NL**]:

$$\begin{aligned} E_{nl}[\mu, \mathbf{u}] = \sum_{k=1}^{N} \int_{\Omega} |I_k(. + u_k) - \mu|^2 dx + \lambda_s \int_{\Omega} \int_{\Omega} w(x, y) |u_k(x) - u_k(y)|^2 dx dy \\ + \lambda_t \int_{\Omega} \int_{\Omega} \hat{w}(x, y) |v_k(x) - v_k(y)|^2 dx dy \end{aligned} \tag{2}$$

The first regularization term is a *spatial* penalty, on the motion fields $\mathbf{u}$, which captures correlations in the motion field between '*non-local*' regions. The second regularization is a *temporal* penalty term which captures the non-local spatial correlations of velocity $v_k = u_{k+1} - u_k$. The above term captures temporal trend of motion across non-local pixels which would help NRR in the case of noise, large motion, low contrast etc.. Also, the temporal penalty is less restrictive on the motion fields than the spatial penalty since only spatial variations in velocity are penalized. $\lambda_s, \lambda_t$ are scalars that balance the terms. $w(x, y), \hat{w}(x, y)$ are weight functions that are used to set the active pixels $y$ that are correlated with the current pixel $x$. For simplicity, we have used a $L2$ metric for the regularization term and a straight forward Gaussian choice for the weight functions $w(x, y) = G_{\sigma}(|x - y|), \hat{w}(x, y) = G_{\hat{\sigma}}(|x - y|)$. To minimize Eq. 2, we use time descent given by the EL and discretized using semi-implicit finite differences, in a multi-resolution framework. For gaussian weights $w, \hat{w}$, the descent equation involves just convolutions which is fast to compute. Also, the descent equation contains linear terms which can be posed in simple implict schemes for fast convergence.

In Fig 1, we show experiments on two synthetic examples which have a combination of noise, large motion and presence of small structures as in PET data. The top row in both examples shows 4 images we want to register. The bottom row shows the resulting mean using [**GW**], [**GW-zD**], and proposed [**GW-NL**].

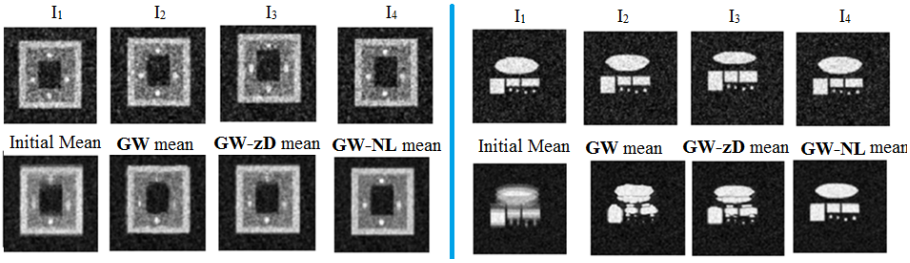


**Fig. 1.** Robustness comparison of [**GW**], [**GW-zD**], [**GW-NL**] in the presence of large motion, noise and small structures. Resulting mean images are shown at the bottom row with [**GW-NL**] giving the best results.

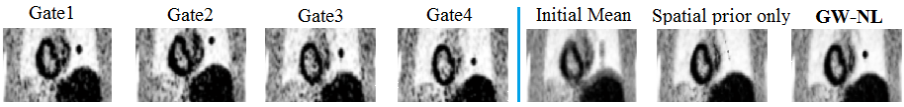


**Fig. 2.** Role of Temporal term in [**GW-NL**]: Better recovery of motion than just using the spatial penalty term.

It is clear from the illustrations that [**GW-NL**] is able to preserve integrity of small structures and handle the challenges of large motion/noise. Fig. 2 highlights the need for the temporal penalty term in [**GW-NL**]. With just the spatial penalty term, i.e. $\lambda_t = 0$ in Eq. 2, we see in a case of extreme motion, the lesion has collapsed.

## 3 Experiments

We present results on 20 datasets which were acquired using a GE Discovery 600 PET-CT system. These data were phase matched with acquired cine CT and reconstructed to form gated PET images (typically 4 to 6 gates). Comparisons of proposed approach [**GW-NL**] is performed with pair-wise NRR [**PW**] available in ITK (Vemuri et al. [12], used for PET motion correction [4]). Next, we compare against Groupwise NRR with zero-deformation penalty (as in [6]) [**GW-zD**]. For [**GW-zD**], we have used the formulation, Eq 1, augmented with the zero-deformation penalty, and minimized using steepest descent.

### 3.1 Illustrative Examples on Two PET Cases

In Fig. 3, we look at qualitative comparisons on 2 gated PET cases, each with 4 gates. For the first PET data example, the data is shown gate-wise (top row), the mean of the gates is shown in the last column. This case exhibits a few challenges. The right lung lesion exhibits large motion (relative to lesion size). The other challenge is contrast variations which are seen in Gate 4. Also, features in the

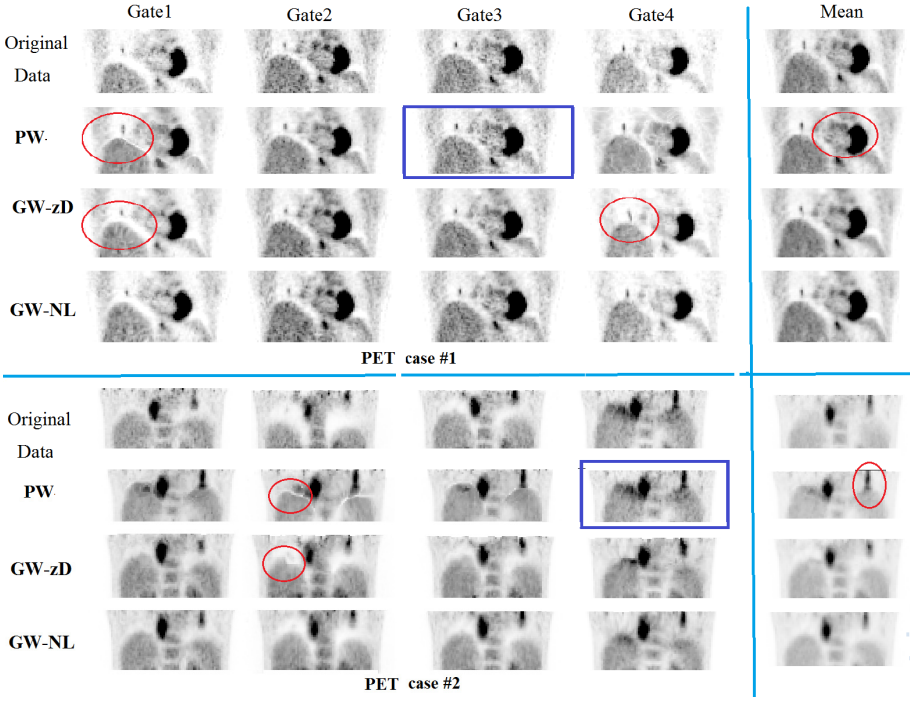


**Fig. 3.** Comparison on 2 PET example cases: [**GW-NL**] has handled the motion/data challenges better than [**PW**], [**GW-zD**]. Artifacts are highlighted by the red circle. The reference gate for [**PW**] is highlighted by the blue rectangle.

cardiac region are not consistently visible in all the gates. The second to fourth rows shows results (registered gates and resultant mean) using [**PW**], [**GW-zD**], and [**GW-NL**] respectively. The [**PW**] approach suffers from registration artifacts in Gates 1 and 4. The effect of bias to reference for [**PW**] is clearly seen in the 2nd gate where distinct features in the cardiac region have collapsed since the reference image (the 3rd gate) does not have it. In the second PET data illustration in Fig. 3, [**PW**] shows similar artifacts due to large motion in the 2nd gate. The issue of bias to reference is also seen here, where in, the lesion on the top of left lung looks more like the reference image (gate 4 in this case). [**GW-zD**] has done reasonably well with minor artifacts due to large motion (highlighted by the red circles). For both examples, as seen in Fig. 3, the proposed approach [**GW-NL**] has handled the challenges highlighted above and shows clean results in the registered gates and the resultant mean image.

A note on timing comparison between the methods. For a gated PET dataset (126x128x47x6), [**PW**] took 90 sec, [**GW-zD**] took 65 sec, and [**GW-NL**] took 80 sec, for convergence. The timing for [**GW-NL**] is quite remarkable considering the noticable improvement in results. Note that, [**PW**], [**GW-zD**], and [**GW-NL**] are all implemented in C++, using standard libraries from ITK.

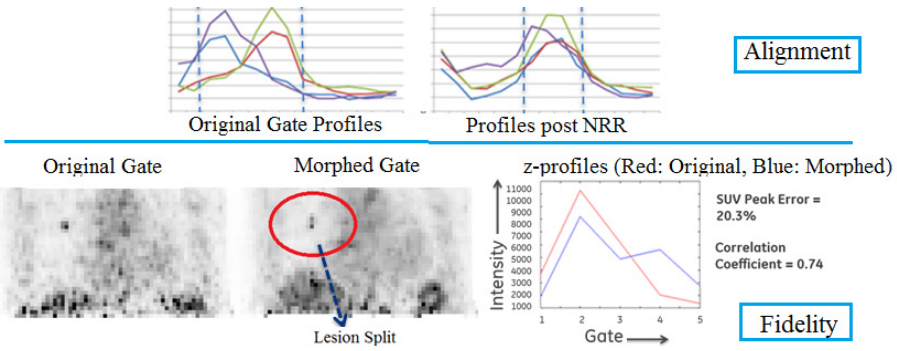


**Fig. 4.** Top row: Alignment metric measures spread in extrema locations of gate profiles (curves shown in the plot). Bottom row: Fidelity metrics (SUV peak, profile correlation) used to measure closeness of lesion profile before and after NRR, to catch artifacts. E.g. The lesion split results in a z-profile (blue curve) with 2 peaks and is captured by the reduced correlation value with the gate profile (red curve)

### 3.2 Quantitative Validation

Here, we use validation based on lesions which are key clinical features in PET data. For this purpose, lesion location was manually annotated on the RRA (average of motion corrected gates) and on each of the original gates of 20 clinical datasets.

Most of validation of NRR is around measuring alignment and very few works (e.g. NIREP, [13]) address artifacts introduced by NRR. Measuring the fidelity/artifacts of registration is very challenging and use of general purpose metrics such as Jacobian of the deformation field might not completely be representative of NRR quality in noisy data as in PET. For gated PET NRR, as discussed in the previous subsection, we want to look at 3 types of artifacts (e.g. see results of [**PW**] in Fig 3), namely, a) stretch type artifacts due to large motion, b) splits, collapse of lesions, and c) bias in results introduced due to artifacts in some gates (we term this as *NRR bias*). While it is difficult to measure the above artifacts in general cases, it is relatively straightforward to do it for lesions. Since lesions remain close to rigid under physiological motion, it is fair to expect lesions to preserve their intensity and shape, post NRR. Thus, to measure both alignment and artifacts(fidelity), we introduce metrics linked to the *z-profiles* of lesions. Since the motion in PET gates is mostly due to respiration, the z-profile (a 1D profile of intensity values in z direction passing through the lesion centroid) characterizes the lesion motion.

The *alignment* of the gates post NRR can be deduced by capturing the spatial spread (using standard deviation) of high intensity values in the z-profiles across all gates (Fig 4, Top row). The better the alignment, the tighter the spread of high intensity values in the ensemble. To capture *fidelity* (Fig 4, Bottom row), we first compute percentage difference between the z-profile peaks of gates

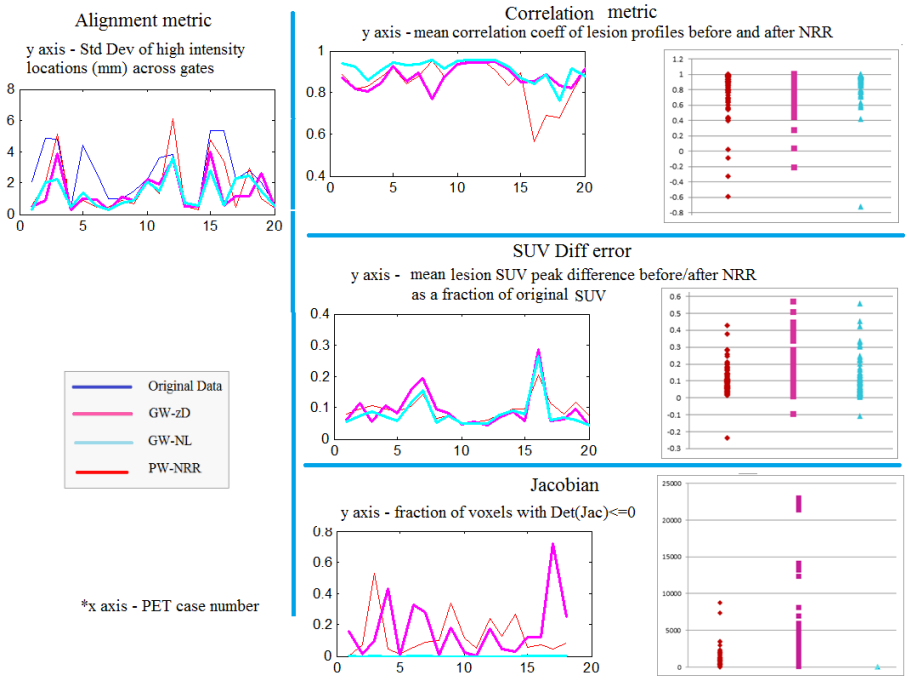


**Fig. 5.** Quantitative comparison on 20 PET Datasets with ≈120 gates in total. Note on metric values: Alignment: lower better, Correlation: higher better, SUV error: lower better, Jacobian: lower better. Left column: Mean across gates for alignment values for 20 cases, Middle column: Mean across gates for fidelity metric values for 20 cases. Last Column: scatter plot of the fidelity metric values across all gates from all cases. The plots show similar alignment, and better fidelity values for [**GW-NL**].

before and after NRR (*SUV peak* error). The SUV peak error indicates whether intensity values in the original gates have been flattened by NRR. Next, we compute *correlation of z-profiles* of individual gates before and after NRR. The correlation coefficient would be high if there is not much of a deviation in the shape of the z-profile post NRR. The above metric can capture issues of lesion splits/collapse and NRR bias to outlier gates. Lastly, to capture artifacts in general at any location, we use *Jacobian* of motion fields to capture crossovers and stretch artifacts (i.e. where $\text{Det(Jac)} \leq 0$).

The quantitative results on 20 PET cases are shown in Fig 5. The data had a good mix of cases with varying lesion motion and noise. A few cases showed motion almost twice the lesion size, in addition to deviation in SUV values as much as 40 % of the mean SUV value across gates. From the alignment plot (Low value indicates good alignment), we see that [**GW-zD**](Magenta), [**GW-NL**](cyan) show better alignment than [**PW**](Red). In the fidelity (correlation, SUV, Jacobian) plots, the first column has the mean metric values across gates,

for each PET case. The last column shows scatter plots of metric values for all gates across the 20 PET cases. The correlation plots (High value indicates good fidelity of lesion shape) show least lesion artifacts for [**GW-NL**]. The SUV peak difference (measures change in SUV, post NRR) is comparable for [**PW**], [**GW-NL**], and slightly higher for [**GW-zD**]. Finally, the Jacobian plot (showing number of voxels with $\mathrm{Det(Jac)} \leq 0$), indicative of amount of crossovers and tears is close to zero for [**GW-NL**], overwhelmingly lesser compared to [**PW**], [**GW-zD**]. To summarize, [**GW-NL**] is seen to be comparable in alignment to the other 2 methods, but has resulted in reduced NRR artifacts.

## 4 Conclusion

Robust NRR for gated PET is key to accurate quantitation. Here, we have captured non-local correlations in motion within the group-wise NRR framework. This has clearly resulted in stability of solutions, robustness to large motion, noise and small structure challenges of PET data. Our results are quantitatively compared with related works using lesion based validation metrics, on 20 cases.

## References

1. Manjeshwar, R.M., Xiaodong, T., et al.: Motion compensated image reconstruction of respiratory gated pet/ct. In: ISBI (2006)
2. Blume, M., Martinez-Moller, et al.: Joint reconstruction of image and motion in gated positron emission tomography. TMI, 1892–1906 (2010)
3. Dawood, M., Buther, F., Schafers, X.J., Respiratory, K.: motion correction in 3d pet data with advanced optical flow algorithms. In: TMI (2008)
4. Wollenweber, S.D., et al.: Eval. of the accuracy and robustness of a motion correction algorithm for pet using a novel phantom approach. In: TNS (2012)
5. Joshi, S., Davis, B., Jomier, M., Gerig, G.: Unbiased diffeomorphic atlas construction for computational. NeuroImage (2004)
6. Bhatia, K.K., Hajnal, J.V., Puri, B.K., Edwards, A.D., Rueckert, D.: Consistent groupwise non-rigid registration for atlas construction. In: ISBI (2004)
7. Wu, G., Jia, H., Wang, Q.: Sharpmean groupwise registration guided by sharp mean image and treebased registration. NeuroImage (2011)
8. Wang, Q., Wu, G., Yap, P.-T., Shen, D.: Attribute vector guided groupwise registration. NeuroImage (2010)
9. Metz, C.T., Klein, S., et al.: Nonrigid registration of dynamic medical imaging data using ndt bsplines. In: MIA (2010)
10. Werlberger: Motion estimation with non-local total variation regularization. CVPR 13, 234–778 (2010)
11. Thiruvenkadam: Dense multi-modal registration with structural integrity using non-local gradients. In: VISAPP (2013)
12. Vemuri, B.C., Ye, J., et al.: Image registration via level-set motion, applications to atlas-based segmentation. In: MMBIA (2003)
13. Christensen, G.E., Geng, X., Kuhl, J.G., Bruss, J., Grabowski, T.J., Pirwani, I.A., Vannier, M.W., Allen, J.S., Damasio, H.: Introduction to the Non-Rigid Image Registration Evaluation Project (NIREP). In: Pluim, J.P.W., Likar, B., Gerritsen, F.A. (eds.) WBIR 2006. LNCS, vol. 4057, pp. 128–135. Springer, Heidelberg (2006)